EPJ manuscript No.
(will be inserted by the editor)

Measurement of Orthopositronium Decay Rate Using SiO_2 Powder: Integration of Thermalization into Time Spectrum Fitting Procedure

O. Jinnouchi, S. Asai and T. Kobayashi

International Center for Elementary Particle Physics, University of Tokyo, Faculty of Science Building 1, 7-3-1 Hongo, Bunkyo-ku, Tokyo, 113-0033, Japan
(e-mail: jinnai3@icepp.s.u-tokyo.ac.jp)

July 8, 2000

Abstract. The intrinsic decay rate of orthopositronium (o-Ps) formed in SiO_2 powder was measured using a modified method which determined the time dependence of the pick-off annihilation rate using high-energy-resolution germanium detectors. That is, the main systematic error due to thermalization was accounted for and integrated into the time spectrum fitting procedure. The averaged value was found to be $\lambda_{\text{o-Ps}} = 7.0399^{+0.0020}_{-0.0021}(stat.) \pm 0.0015(sys.)\mu s^{-1}$, which agrees well with the $O(\alpha^2)$ QED prediction; varying 3.3-4.7 experimental standard deviations from other measurements.

PACS. 36.10.Dr Positronium, muonium, muonic atoms and molecules – 11.10.St Bound and unstable states, BetheSalpeter equations – 12.20.Fv Experimental test

1 Introduction

1.1 o-Ps lifetime problem

The bound state of an electron and positron, positronium (Ps), is a pure quantum electrodynamical system that provides a highly sensitive field for testing accurate descriptions of bound states in quantum field theory. The triplet (1^3S_1) state of Ps, orthopositronium (o-Ps), will in most cases decay into three photons due to having odd-parity under the C-transformation. Accordingly, the decay lifetime is sufficient such that direct, precise measurements [1–3] have indicated that the o-Ps decay rate is much larger, i.e., 1670, 1600, and 1170 ppm respectively, than the theoretical QED prediction (7.039934(10) μs^{-1}) corrected up to $O(\alpha^2)$ [4–13]. These respective discrepancies of 9.1, 8.0, and 5.2 experimental standard deviations are statistically significant, being referred to as the 'o-Ps lifetime problem.'

Although a variety of experiments have since been carried out to search for exotic decay modes of o-Ps [14–20], none have provided confirming evidence to elucidate this discrepancy.

1.2 Thermalization of o-Ps

We went on to perform further study [21] in which two independent precision measurements were carried out using two types of SiO_2 powder. Results correlated well, giving a combined value of

$$\lambda_{\text{o-Ps}} = 7.0398 \pm 0.0025(stat.) \pm 0.0015(sys.)\ \mu s^{-1},$$

which is consistent with the QED $O(\alpha^2)$ prediction. This measurement employed a completely new method that took into account the thermalization process of o-Ps.

Since some fraction of o-Ps inevitably results in 'pick-off' annihilations due to collisions with atomic electrons of the target material, the observed o-Ps decay rate λ_{obs} is the sum of the intrinsic o-Ps decay rate $\lambda_{3\gamma}$ and the pick-off annihilation rate λ_{pick}, i.e.,

$$\lambda_{obs}(t) = \lambda_{3\gamma} + \lambda_{pick}(t), \tag{1}$$

where λ_{pick} is proportional to the collision rate of o-Ps with the target materials; hence being proportional to the densities of the target materials and the velocity of o-Ps.

Immediately after formation, o-Ps has a kinetic energy of about 1 eV, thermalizing via elastic collisions with surrounding molecules to an ultimate thermal energy of about 0.03 eV. Due to the deceleration or thermalization process, λ_{pick} must be described as a function of time dependent on the properties of the respective materials. λ_{obs} was previously measured [1–3] by varying the densities of the target materials, with the extrapolation to zero densities expected to yield $\lambda_{3\gamma}$ under the assumption of constant o-Ps velocity. Unfortunately, however, such extrapolation results in large systematic error due to an expected low thermalization rate, especially regarding the low density limit. Measurements in SiO_2 powder indicated this systematic problem [21,22]; while in other experiments, o-Ps thermalization rates measured in gas were also substantially smaller than previously thought [23]. Another problem is that the assumption of linear dependence of λ_{pick} on the densities of the target materials is not always valid, i.e., o-Ps collisions with materials could very well be more complex due to the occurrence of multiple scattering at material surfaces.

Therefore, our previous measurements adopted a formulation containing all information representing the thermalization process [21] ; hence completely removing systematic errors related to the thermalization process. From Eq. (1), the population of o-Ps, $N(t)$, can be expressed as

$$N(t) = N_0 \exp\left(-\lambda_{3\gamma}\int_0^t\left(1+\frac{\lambda_{pick}(t')}{\lambda_{3\gamma}}\right)dt'\right). \quad (2)$$

Note that the energy distribution of photons from the 3-body γ-decay is continuous below the steep edge at 511 keV, whereas the final state of the pick-off annihilation is 2-body; a behavior producing the 511-keV monochromatic peak. If the energy and timing information are simultaneously measured, $\lambda_{pick}(t)/\lambda_{3\gamma}$ can be determined from the energy spectrum of the emitted photon. Then, providing the ratio is determined as a function of time, the intrinsic o-Ps decay rate $\lambda_{3\gamma}$ can be directly obtained by fitting the observed time spectrum with Eq. (2); an approach which precludes any ambiguity due to the thermalization process.

2 Experimental setup

2.1 Uncertainties in previous measurements

Although our 1995 results were consistent with QED predictions, the error was large in comparison with that of other experiments [1–3]. The time spectrum was obtained using CsI(Tl) scintillators which provided a relatively broad time response function ($\sigma\sim4$ ns) and long scintillation decay time. Accordingly, since some fraction of the prompt annihilation may have flown into the o-Ps decay region, uncertainties occurred in the time spectrum range immediately after the prompt events. This uncertainty led a restriction in the statistics such that we obtained a rather large error.

Here, although a new experimental setup/technique is used similar to the previous one, the above-mentioned problems are mitigated by employing NaI(Tl) versus CsI(Tl) scintillators.

2.2 Apparatus

Figure 1 shows the experimental setup, where a very weak ^{22}Na β positron source (0.08 μCi) with 2-mm spot diameter is sandwiched between two sheet-type plastic scintillators (NE104) having a 12-mm diameter and 100-μm thickness. The source, held by a cone made of 25-μm-thick aluminized myler, is situated at the center of a 48-mm diameter vacuum chamber made of 500-μm-thick glass. The chamber, evacuated to 4×10^{-2} torr, is filled with SiO_2 silica powder (density, 0.03 g/cm^3) having a grain size of 7-nm in diameter.

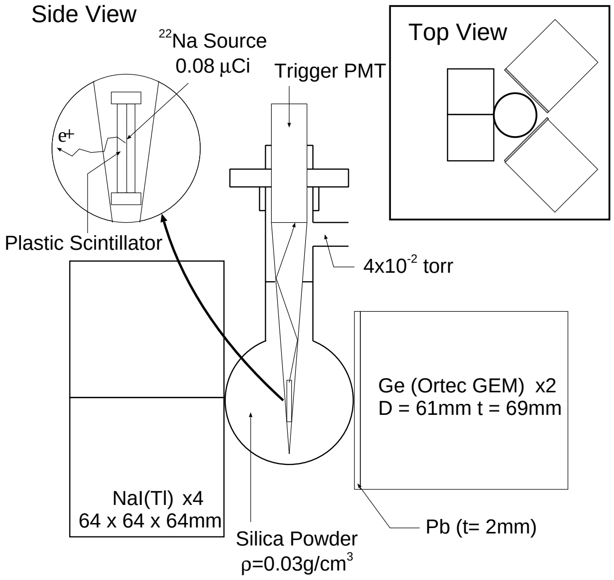

Fig. 1. Experimental setup.

Most emitted positrons passing through the scintillators transmit a light pulse to a trigger photo-multiplier (PMT) (Hamamatsu H-3165-04) such that Ps is formed as the positrons are stopped in the silica powder. The photons subsequently emitted by the decay of o-Ps are measured using two types of detectors.

Two germanium semiconductor detectors (diameter, 61 mm; thickness, 69 mm; Ortec, GEM 38195) precisely determine $\lambda_{pick}(t)/\lambda_{3\gamma}$ as a function of time. The detectors are arranged perpendicular to each other (Fig. 1) to reduce the incidence of Compton scattered photons from the other detector. A 2.0-mm-thick lead sheet located in front of the detectors eliminates the contribution of the two simultaneous low-energy photons produced by the 3γ-decay of o-Ps. Due to the detector's excellent energy resolution, i.e. ,1.78 keV FWHM at 1274.6 keV, the resultant energy spectrum allows the monochromatic 2γ pick-off annihilation to be easily distinguished from the continuous 3γ-decay.

The four NaI(Tl) scintillators (crystal size, 64x64x64 mm) simultaneously obtain time and energy information. Because they have much higher efficiencies compared to the Ge detectors, while also having good time response functions, the obtained time spectrum can be fit to Eq. (2).

2.3 Electronics

Trigger PMT output is fed to a discriminator which provides the start signal for both time-to-digital converters (TDCs) (Hoshin C006 and CAEN C414) and the reset signals for other electronics blocked (vetoed) during measurements. The TDCs are calibrated by a time-calibrator (Ortec 462) having an intrinsic time accuracy of 50 *ppm*.

One output from the Ge detector preamplifier is fed into a fast-filter amplifier (FFA)(Ortec 579) whose output is divided into three signals by a linear fan-out module (LFF)(Lecroy 428F). One signal feeds a constant-fraction discriminator (CFD)(Ortec 473A) whose output is used as the stop signal for the TDC, while the other two feed a charge-sensitive analogue-to-digital converter (C-ADC) (Lecroy 2249SG). This enables measuring energy with a narrow gate width (1.25 μs) and the base-line condition just prior to an event having a 200-ns ADC gate width. The differential and integral time of the fast-filter amplifier are optimized to obtain good time resolution of 6 ns rms. To measure a precise energy spectrum, the other output from the preamplifier is amplified by a spectroscopy amplifier (Ortec 673) such that shaped signals are fed into a peak-holding amplitude-to-digital converter (PH-ADC) (Hoshin C011) with 40-μs gate width.

The output from each of the four NaI(Tl) scintillators is divided by the LFF into four signals. One output is fed into a discriminator whose output with good time resolution of 1.2 ns rms provides the stop signal for the TDCs, while the other three outputs are fed to C-ADCs. One C-ADC with 3-μs gate width, called the *wide ADC* (Lecroy 2249W), measures the whole charge for the duration of the signal; one with 250-ns gate width, called the *narrow ADC* (Lecroy 2249SG), measures the charge itself; and one with 180-ns gate width, called the *base ADC* (Lecroy 2249SG) measures the base-line condition of the signal just prior to the event.

Accordingly, each Ge detector and NaI(Tl) scintillator provides three types of ADC information. Because pile-up events result in larger charge integration on the *wide* versus *narrow ADC*, their values are compared such that these events are effectively rejected. The *base ADC* is also used to reject pile-up events which can occur if the base-line condition is shifted due to any remaining tail of the previous signal. All ADCs use entirely independent gate input such that they are able to start charge integration using self timing, which results in the ADC gate width being narrower in accordance with signal duration.

Room temperature was maintained within $\pm 0.5°C$ to ensure stability of the amplifiers, ADCs, and TDCs.

3 Analysis

Use of the energy spectrum precisely measured by the Ge detectors enables determining $\lambda_{pick}(t)/\lambda_{3\gamma}$. The energy spectrum of the photon originating from the pure o-Ps sample is obtained by subtracting the accidental contribution (time range, $2000 - 3000 ns$) from the measured spectrum. Figure 2 shows the resultant o-Ps spectrum, where the pick-off annihilation peak at 511 keV is clearly evident at the edge of the 3γ-decay continuous spectrum.

Using Monte Carlo simulation in which the setup geometry and various material distributions are reproduced

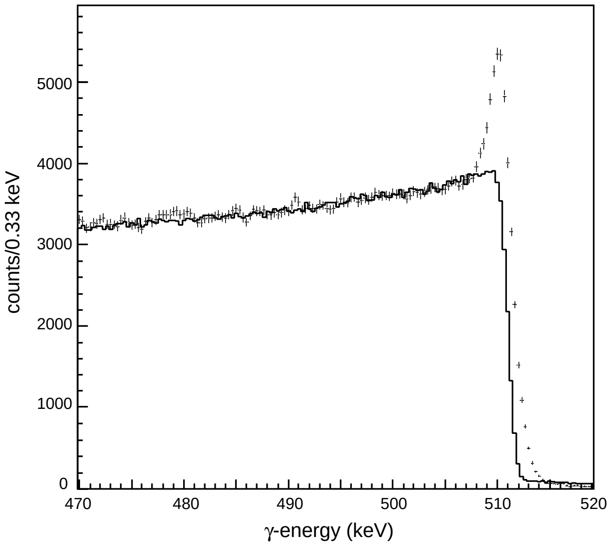

Fig. 2. Energy spectrum of o-Ps decay obtained by Ge detectors using a time window of $160 - 710$ ns. The solid line indicates the 3γ-decay spectrum calculated by Monte Carlo simulation, agreeing well with measured data below 508 keV.

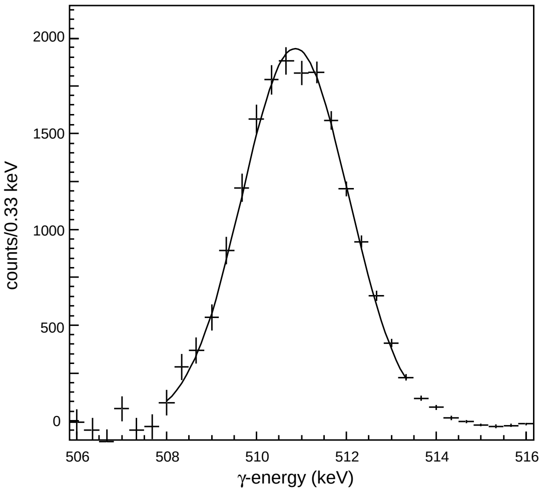

Fig. 3. Enlarged view of measured spectrum after subtracting the 3γ contribution from the o-Ps spectrum.

in detail allowed us to calculate the expected 3γ-decay energy spectrum. That is, for every simulated event, three photons are generated according to an $O(\alpha)$ corrected energy spectrum, with successive photoelectric, incoherent, or coherent scattering interactions of every photon with materials being followed until all photon energy is deposited. The response function of the detector is determined based on the measured spectrum of monochromatic γ-rays emitted from ^{152}Eu(344.3 keV), ^{85}Sr(514.0 keV), and ^{137}Cs(661.7 keV), the lines of which are convoluted in the simulation.

As shown in Fig. 2, the o-Ps and 3γ spectra indicate good agreement below 508 keV. Although the simulation produced a detailed structure of the actual experimental setup, the shape of the 3γ spectrum is nearly independent of simulation details in that the sharp drop-off at 511 keV

is solely due to the phase-space cutoff, being almost entirely determined by the energy response function of the Ge detectors. Figure 3 shows an enlarged view of the o-Ps spectrum after subtracting the 3γ spectrum, where the resultant spectrum peak and measured Ge detector response function fit well. Since the center of the fitted peak is located at $510.86 \pm 0.21\ keV$, this indicates that subtraction of the 3γ contribution is properly performed. Hence, the peak is considered to represent a pure sample of pick-off annihilations, and the number of pick-off annihilations can be counted. The number of decays of o-Ps into 3γ's can accordingly be counted using the o-Ps spectrum such that $\lambda_{pick}/\lambda_{3\gamma}$ is simply estimated from the counts ratio, where $n_{pick}/n_{3\gamma}$ is multiplied by a normalization factor considering relative efficiencies of the Ge detectors and the $O(\alpha)$ corrected energy spectrum. Since $\lambda_{pick}/\lambda_{3\gamma}$ is only dependent on the relative efficiencies of the Ge detectors vice absolute efficiencies, the resultant ratio is stable against various systematic errors.

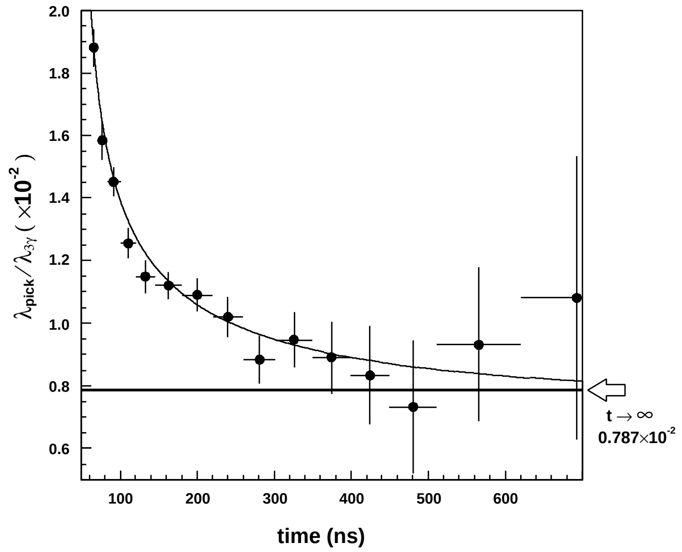

Fig. 4. Pick-off annihilation rate and 3γ decay rate plotted as a function of time. Fitting results (solid line) are obtained using Eq. (4). The horizontal line at $\lambda_{pick}/\lambda_{3\gamma} = 0.787 \times 10^{-2}$ shows the approximate value at $t \to \infty$.

$\lambda_{pick}/\lambda_{3\gamma}$ ratios are respectively calculated in the same manner using various time windows, with Fig. 4 showing time dependencies of these values. Because the fractional energy loss of o-Ps per collision is dependent on its energy in SiO_2 powder, the time dependence of the average kinetic energy of o-Ps at time t, $\overline{E(t)}$, can be expressed by the following differential equation [24,25]:

$$\frac{d}{dt}\overline{E(t)} = -\sqrt{2m_{Ps}\overline{E(t)}} \times \left(\overline{E(t)} - \frac{3}{2}k_B T\right)\left(\frac{2}{\overline{M}\ \overline{L}}\right)\sum_{j=0}^{\infty} a_j \left(\frac{\overline{E(t)}}{k_B T}\right)^{j/2}, \quad (3)$$

where m_{Ps}, $\overline{M}$, and $\overline{L}$ are the mass of o-Ps, effective mass at the surface of the SiO_2 grain, and mean distance between the grains. Since the pick-off annihilation rate is proportional to the average velocity of o-Ps, $\lambda_{pick}/\lambda_{3\gamma} (\equiv \theta(t))$ can be expressed as

$$\frac{d}{dt}\theta(t) = -C\left(\theta(t)^2 - \theta_\infty^2\right)\sum_{j=0,1,2,\cdots} a_j \theta(t)^j, \quad (4)$$

where $\theta_\infty \equiv \theta(t \to \infty)$, C, and $a_j (j = 1, 2, \cdots)$ are constants. With the exception that the summation term is replaced with abbreviated form $\theta(t)^\kappa$ in which κ is an arbitrary real number, Eq. (4) is used for fitting measured $\lambda_{pick}/\lambda_{3\gamma}$ values. As indicated by the results in Fig. 4, o-Ps takes about 600 ns to become well thermalized in SiO_2 powder.

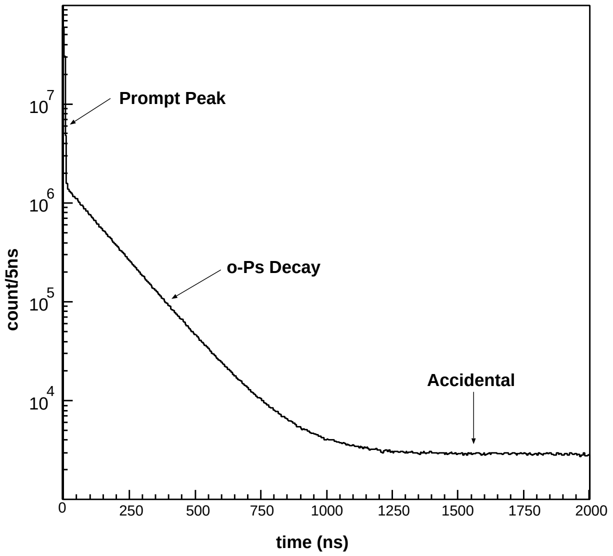

Fig. 5. Time spectrum of NaI(Tl) scintillators with a photon energy window of 350-450 keV.

Figure 5 shows the time spectrum of NaI(Tl) scintillators using a photon energy window of $350 - 450\ keV$, where the sharp peak from prompt annihilations is followed by exponential decay of o-Ps and the flat spectrum of accidental events. Due to using a weak positron source ($0.08\ \mu Ci$), the o-Ps decay curve covers a wide region of about $1.2\ \mu s$, being about eight times as long as the o-Ps lifetime.

Using the least square method the time spectrum is fitted with

$$F(t) = \exp(-R_{stop}t)\left[\left(1 + \frac{\epsilon_{pick}}{\epsilon_{3\gamma}}\frac{\lambda_{pick}}{\lambda_{3\gamma}}\right)N(t) + C\right], \quad (5)$$

where $N(t)$ is in Eq. (2), and ϵ_{pick} and $\epsilon_{3\gamma}$ are respectively the probabilities that the photons emitted from the pick-off annihilation and 3γ-decay of o-Ps deposit energy of $350 - 450\ keV$ in the NaI(Tl) scintillators. Results of Monte Carlo simulation estimated $\epsilon_{pick}/\epsilon_{3\gamma}$ to be

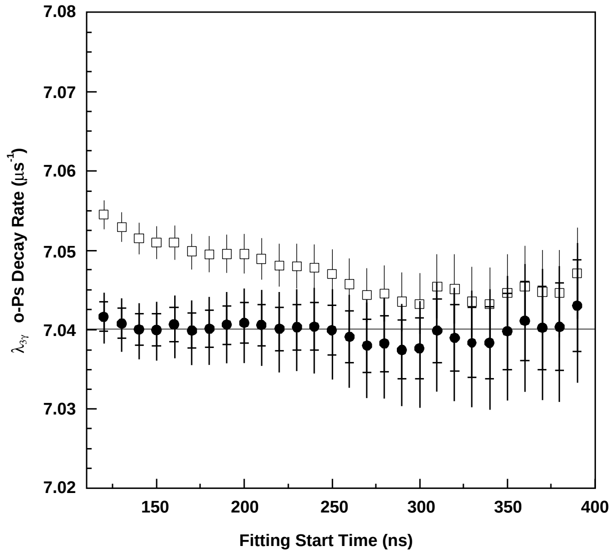

Fig. 6. Decay rate of o-Ps plotted as a function of fitting start time. Open squares and closed circles show values obtained by fitting with Eq. (6) and the proposed method, respectively, while the horizontal line shows the value obtained at the start of fitting (140 ns).

0.128 ± 0.002, while R_{stop} is the measured stop rate of the NaI(Tl) scintillators.

Open squares in Fig. 6 show fitted values of the decay rate of o-Ps, $\lambda_{3\gamma}$, plotted as a function of fitting start time using a simple exponential function, i.e.,

$$f(t) = \exp(-R_{stop}) \left[\, N_0 \exp\left(-\lambda_{obs} t\right) + C \, \right]. \qquad (6)$$

Since observed λ_{obs} contains the pick-off rate fraction, the intrinsic decay rate $\lambda_{3\gamma}$ is obtained by correcting λ_{obs} by a factor of $(1+\lambda_{pick}(t \to \infty)/\lambda_{3\gamma}) \approx 1.00787$. Closed circles in Fig. 6 show fitting results obtained using the proposed method, where the obtained values are stable against the fitting start time. Figure 6 shows the effect due to thermalization has been completely taken into account in our new method. The horizontal error-bars indicate statistical errors solely due to fitting the NaI(Tl) time spectrum, while the vertically extending bars represent propagated errors due to the fitting of $\lambda_{pick}(t)/\lambda_{3\gamma}$. Note the stable range after 140 ns, where the tail effect of prompt events is negligible; hence this time is used as the fitting start time. The resultant value is $\lambda_{3\gamma} = 7.0401\,^{+0.0033}_{-0.0038}\,(stat.)\,\mu s^{-1}$, which includes the statistical error in determining $\lambda_{pick}(t)/\lambda_{3\gamma}$.

When systematic errors were estimated for various effects, the predominate contribution was found to be due the Monte Carlo simulation. That is, the 3γ contribution in the o-Ps spectrum is estimated by normalizing the Monte Carlo distribution with measured data from $480 - 505$ keV. In this measurement, we used the same Monte Carlo code adopted previously [21]. Equivalent systematic errors originating from the simulation are accordingly expected and estimated to be $+190$ and -150 ppm. Other errors arise due to in-uniformity of SiO_2 powder (± 30 ppm), fluctuations in relative efficiencies of Ge detectors dependent on the position of o-Ps formation (-40 ppm), and the position of o-Ps decay (-50 ppm). The remaining sources of error are due to hardware considerations: the absolute accuracy of the time calibration (± 50 ppm), uncertainties in the relative efficiencies of the Ge detectors (± 50 ppm), dependence on the base-line condition of NaI scintillators (± 23 ppm), and relative efficiency of the NaI scintillators ($\epsilon_{pick}/\epsilon_{3\gamma}$) ($\pm 7$ ppm). Since these systematic errors are independent of each other, the total systematic error is their quadratic sum.

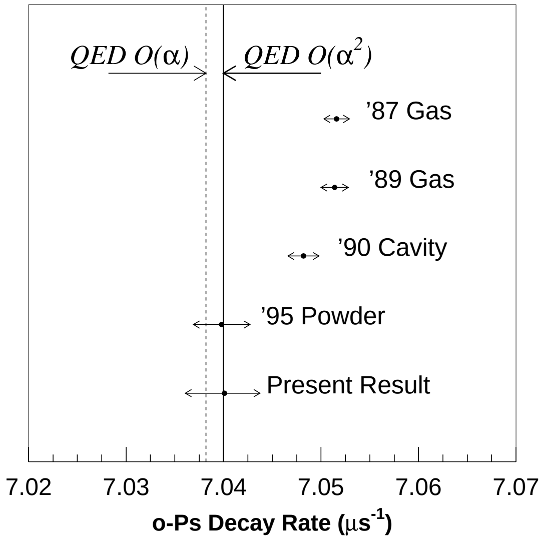

Fig. 7. History of the measurement of o-Ps decay rate. The solid line shows $O(\alpha^2)$ corrected QED prediction, while the dashed line shows $O(\alpha)$ corrected value.

The obtained result is $\lambda_{3\gamma} = 7.0401\,^{+0.0033}_{-0.0038}\,(stat.)\,^{+0.0015}_{-0.0014}\,(sys.)\,\mu s^{-1}$. Although the obtained precision is relatively lower compared to previous experiments, the results are essentially consistent as shown in Fig. 7 which indicates the history of o-Ps decay rate measurements. In addition, substantial improvement in the timing system is demonstrated.

4 Conclusions

The o-Ps decay rate was measured in SiO_2 powder using a modified method in which the effect of thermalization of o-Ps is accounted for by high energy-resolution Ge detectors. By combining obtained and our previous result [21] that assume systematic errors mainly stem from the same origins, we obtained $\lambda_{3\gamma} = 7.0399\,^{+0.0020}_{-0.0021}\,(stat.) \pm 0.0015(sys.)\mu s^{-1}$. This is consistent with the $O(\alpha^2)$ corrected QED prediction of $7.039934(10)\mu s^{-1}$[13] within an error of 360 ppm, while varying $3.3 \sim 4.7$ σ from other recent measurements [1–3]. Realizing that this experiment represents dynamic development, further improvement in Ge timing response is expected soon; an innovation that should enable us to investigate the fast component preceeding a 140-*ns* start time such that the $O(\alpha^2)$ contribution in QED can be ultimately be confirmed at a level of just 200 *ppm*.

Sincere gratitude is extended to Professor Toshio Hyodo and Dr. Yasuyuki Nagashima, University of Tokyo, for their insightful suggestions and valuable discussions concerning o-Ps thermalization.

References

1. C. I. Westbrook, D. W. Gidley, R. S. Conti, and A. Rich, Phys. Rev. Lett. **58**, 1328 (1987).
2. C. I. Westbrook, D. W. Gidley, R. S. Conti, and A. Rich, Phys. Rev. **A40**, 5489 (1989).
3. J. S. Nico, D. W. Gidley, A. Rich, and P. W. Zitzewitz, Phys. Rev. Lett. **65**, 1344 (1990).
4. G. S. Adkins, A. A. Salahuddin, and K. E. Schalm, Phys. Rev. A **45**, 7774 (1992).
5. G. S. Adkins, Phys. Rev. Lett. **76**, 4903 (1996).
6. G. S. Adkins, K. M. Melnikov, and A. Yelkhovsky, hep-ph/9905553, 1999.
7. P. Labelle, G. P. Lepage, and U. Magnea, Phys. Rev. Lett. **72**, 2006 (1994).
8. R. N. Faustov, A. P. Martynenko, and V. A. Saleev, Phys. Rev. A **51**, 4520 (1995).
9. A. P. Burichenko, Phys. At. Nucl. **56**, 640 (1993).
10. W. E. Caswell and G. P. Lepage, Phys. Rev. A **20**, 36 (1979).
11. I. B. Khriplovich and A. S. Yelkhovsky, Phys. Lett. B **246**, 520 (1990).
12. A. I. Milstein and I. B. Khriplovich, JTEP **79**, 379 (1994).
13. G. S. Adkins, R. N. Fell, and J. Sapirstein, hep-ph/0003028, 2000.
14. S. Asai, S. Orito, K. Yoshimura, and T. Haga, Phys. Rev. Lett. **66**, 2440 (1991).
15. S. Orito, K. Yoshimura, T. Haga, M. Minowa, and M. Tsuchiaki, Phys. Rev. Lett. **63**, 597 (1989).
16. S. Asai, K. Shigekuni, T. Sanuki, and S. Orito, Phys. Lett. B **323**, 90 (1994).
17. M. Tsuchiaki, S. Orito, T. Yoshida, and M. Minowa, Phys. Lett. B **236**, 81 (1990).
18. T. Mitsui, K. Maki, N. Muramoto, T. Sato, and S. Asai, Europhys. Lett. **33**, 111 (1996).
19. T. Mitsui, R. Fujimoto, Y. Ishisaki, Y. Ueda, Y. Yamazaki, S. Asai, and S. Orito, Phys. Rev. Lett. **70**, 2265 (1993).
20. S. Asai, S. Orito, T. Sanuki, M. Yasuda, and T. Yokoi, Phys. Rev. Lett. **66**, 1298 (1991).
21. S. Asai, S. Orito, and N. Shinohara, Phys. Lett. **B357**, 475 (1995).
22. S. Asai, *New Measurement of Orthopositronium Lifetime*, Ph. D. thesis, 1994, University of Tokyo.
23. M. Skalsey, J. J. Engbrecht, R. K. Bithell, R. S. Vallery, and D. W. Gidley, Phys. Rev. Lett. **80**, 3727 (1998).
24. Y. Nagashima, T. Hyodo, K. Fujiwara, and A. Ichimura, J. Phys. B **31**, 329 (1998).
25. Y. Nagashima, M. Kakimoto, T. Hyodo, K. Fujiwara, A. Ichimura, T. Chang, J. Deng, T. Akahane, T. Chiba, K. Suzuki, B. T. A. McKee, and A. T. Stewart, Phys. Rev. A **52**, 258 (1995).